Korean J. Chem. Eng., **21**(6), 1108-1118 (2004)

Flow Directions in Gas Assisted Injection Molding When Cavities of Square Flat Plates and Pipes are Involved 1. Theory of Flow Model and Its Criterion

Kwang-Hee Lim†

Department of Chemical Engineering, Daegu University, Kyungsan, Kyungbook 712-714, Korea
(*Received 28 February 2004 • accepted 7 August 2004*)

Abstract−In such a complex situation as the cavity of two square plates connected to cavities composed of four pipes with same length and different diameter connected in series and parallel, the resistance of cavity of two square plates should be combined with that of pipes to determine the gas direction in gas assisted injection molding (GAIM). The flow model of Newtonian fluid was previously suggested under the fan-shaped geometry incuding relatively thin cavity of two square plates when $\rho\bar{v}_r H/\mu(H/R_0) \ll 1$, $(H/R_0)^2 1/\hat{\theta}^2 \ll 1$ and $(H/R_0)^2 \ll 1$. However, one may frequently encounter the problem of relatively thick fan-shaped cavity between two square plates where $(H/R_0)^2$ is around 10^{-1} and $\hat{\theta}^2$ is the order of one. The rule of thumb containing a first order-approximated flow model by perturbation technique was introduced to show, in qualitative way, whether the resistance of the relatively thick cavity of two square plates may affect the gas direction in GAIM under the fore-said geometry. Subsequently, various simulations were performed under the conditions that all dimensions of cavity of two square plates and pipes were fixed except for the diameters of pipes. The results of simulation were compared with the results of the rule of thumb (RT1) containing the approximated flow model as well as those of another rule of thumb (RT2) without the resistance of the relatively thick cavity of two square plates. The results of simulations were generally consistent with the former in qualitative way to determine gas directions in gas assisted injection molding even though a relatively large value of 0.36 was applied as the value of ε to describe a relatively thick cavity of two square plates. In addition, the situation was treated when cavities of pipes and runners were involved in configuration. The rule of thumb was used for the ratio of initial velocities to be recalculated at the first coming change of diameters when the ratio was close to unity and it was quite consistent to the results of simulation.

Key words: Gas Assisted Injection Molding, Rule of Thumb, Preferred Direction of Gas, The Least Resistance to Initial-resin Velocity

INTRODUCTION

In the gas-assisted injection molding (GAIM), gas should flow towards the intended directions. If gas goes in a wrong direction, many problems occur including a phenomenon called "blow through" and another phenomenon called "penetration into thin walled region." If the gas does not enter where it is expected, a problem like sink mark occurs. The control of gas direction is thus one of the most critical aspects in the application of the technology.

Many researchers [Chen, 1995; Khayat et al., 1995; Chen et al., 1996a, b; Gao et al., 1997; Shen, 1997, 2001; Parvez et al., 2002] have investigated the primary and secondary gas penetration in terms of gas-liquid interface and polymer melt front in GAIM. Chen et al. [1995] performed both experimental investigation and numerical simulation on the characteristics of the secondary gas penetration in a spiral tube during the GAIM. Khayat et al. [1995] simulated the primary gas penetration stage of GAIM process USING Eulerian boundary-element approach. Chen et al. [1996a, b] studied gas and melt flow on GAIM for the design of a thin plate/angle bracket part with a gas channel with numerical simulations using control volume/finite element method. Gao et al. [1997] developed a numerical model capable of predicting the gas penetration using multiple gas-injection units. Shen [1997] develop the model to predict the gas-liquid interface and polymer melt front of generalized Newtonian fluid in GAIM. Later Shen [2001] developed an algorithm for commercial software to predict the polymer melt front, gas front and solid layer in GAIM. Pavrez et al. [2002] carried out computer simulation of the GAIM process using Moldflow, a commercial software and its outcome were compared with the experimental results. However, the method of their approach cannot be regarded as a rule of thumb but was close to the way of commercial software for GAIM in that numerical simulations were performed by the use of control volume/finite element method or boundary-element approach.

It is a well-known rule of thumb that the prerequisite condition for gas flow is the existence of an unfilled region or short shot at the moment of gas injection. "Gas goes to the direction of the last resin fill area" is a very common statement to many GAIM engineers and mold/part designers. Once this unfilled region exists, gas flows to that direction. However, when more than one area exists to fill with resin, a mold design engineer for GAIM technologies has to determine to which direction gas goes that commercial software for GAIM (e.g., Moldflow) may be utilized for its mold design. However, commercial software is generally expensive and is sometimes hard to be familiar with. The goal of this paper is to suggest

†To whom correspondence should be addressed.
E-mail: khlim@daegu.ac.kr

a rule of thumb to predict a gas direction in GAIM that must be very important information. When there exists more than one unfilled region and these paths are competing for the direction of gas, it has been believed that the gas preferred the direction of the least resistance. In other words, during the injection stage the gas usually takes the path of least flow resistance to catch up with the melt front [Chen et al., 1996a, b]. Thus "Gas goes to the direction of the least resistance" has been another common statement for GAIM experts.

The rule of thumb on the direction of gas flow for GAIM has been investigated [Lim and Soh, 1999; Soh, 2000; Soh and Lim, 2002; Lim and Lee, 2003; Lim, 2004a, b; Lim and Hong, 2004] and simulation packages have been used to verify the gas direction predicted by the rule of thumb. Soh [2000] used a pressure drop requirement as a variable for the resistance of gas directions, where the resistance of gas flow was proportional to the pressure drop requirement to keep velocities to both sides same. Upon comparing pressure drops of both sides, gas directions are predicted to the side of the lower pressure drop. In complex situations, however, this method is hardly applicable. Lim and Soh [1999] assumed that the pressure difference between a gas injection point and appropriate vent areas at both sides of well-maintained molds is equal. Consequently, the pressure drops at both sides are equated to compare the resistances and to predict the gas direction.

If the resistance in the sentence of "gas goes to the direction of the least resistance" is the resistance to flow rates, this statement is not always correct. The resistance to flow rates cannot be a criterion in the prediction of gas flow direction in GAIM. Soh [2000] qualitatively treated the special case that the same resistances to flow rates for both sides resulted in the same flow rates for both sides under the geometry that two same sets of two different pipes connected in series are located in parallel. Soh and Lim [2002] suggested the definition of the resistance to velocity to predict the gas-preferred direction under the simplest geometry of two different pipes connected at one connection point. However, if more complicated geometries are involved, the change of velocity of melt resin becomes unavoidable. Therefore, as a rule of thumb, a more developed-precise definition of the resistance to velocity should be established. In such a complex situation as runners or thick cavity of two square plates connected to cavities composed of four pipes with same length and different diameter connected in series and parallel, Lim and Lee [2003] proposed the developed concept of a criterion in the prediction of gas flow direction of GAIM as the resistance of pipes to the initial velocity of melt polymer at the nearest geometry to a gas injection point.

Lim [2004a] proposed a new equation to describe the pressure drop requirement for a steady state flow through a general fan-shaped cavity formed by two parallel plates. Then the definition of a resistance to initial velocity was proposed as a rule of thumb to compare the results of simulation performed by such a commercial software as Moldflow with those of diagnosis on the direction of gas flow using the suggested rule of thumb. Lim and Hong [2004] firstly performed the modeling algebraically on GAIM process by use of both the mass balance of resin in consideration of coated layer including frozen layer and hydrodynamic layer left behind near mold wall and the equation describing pressure drop requirement in order to predict the time-dependent length of gas penetration between gas injection point and moving gas-liquid interface. Lim [2004b] applied

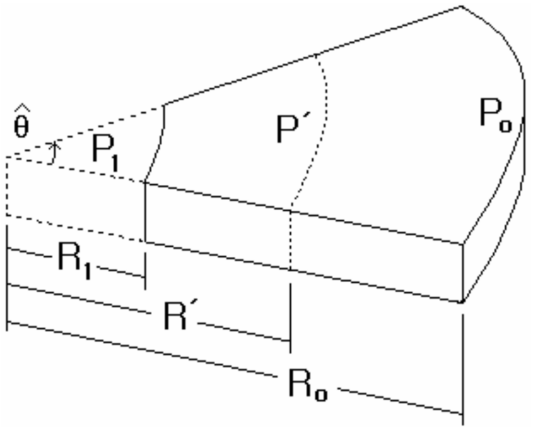

Fig. 1. The flow through between panel areas of fan-shaped geometry where a molten polymer liquid is fed into the mold at $r=R_1$ with the pressure of P_1 and is going out of the mold at $r=R_0$ with the pressure of P_0.

the model on GAIM process previously suggested by Lim and Hong [2004] to various geometries of mold-cavity including that of two square flat plates as well as that of a set of pipes.

In this paper the authors shall combine the resistance of cavity of two square plates with that of pipes to determine the gas direction under the foresaid geometry that Lim and Lee [2003] dealt with. The flow model of Newtonian fluid was previously suggested under the fan-shaped geometry including relatively thin cavity of two square plates when $\rho\bar{v}_r H/\mu(H/R_0)\ll 1$, $(H/R_0)^2 1/\hat{\theta}^2\ll 1$ and $(H/R_0)^2\ll 1$ [Lim, 1999, 2004a]. However, one may frequently encounter the problem of relatively thick cavity between two square-plates where $(H/R_0)^2$ is around 10^{-1} and $\hat{\theta}^2$ is the order of one. For these conditions a first order-approximated flow model and rule of thumbs shall be introduced to show whether the resistance of the relatively thick cavity of two square plates may affect the gas direction in GAIM under the fore-said geometry, and the result of simulation shall be compared with the result of rule of thumb for both conditions.

METHODS

1. Theory

For incompressible fluids, continuity equation in cylindrical coordinates becomes:

$$\frac{1}{r}\frac{\partial}{\partial r}(rv_r)+\frac{\partial v_z}{\partial z}=0 \tag{1}$$

when v_θ is assumed to be zero velocity.

Momentum equation for Newtonian fluid, neglecting gravity, becomes:

$$\rho\left(\frac{\partial v_r}{\partial t}+v_r\frac{\partial v_r}{\partial r}+v_z\frac{\partial v_r}{\partial z}\right)=-\frac{\partial P}{\partial r}+\mu\left[\frac{\partial}{\partial r}\left(\frac{1}{r}\frac{\partial}{\partial r}(rv_r)\right)+\frac{1}{r_2}\frac{\partial^2 v_r}{\partial\theta^2}+\frac{\partial^2 v_r}{\partial z^2}\right] \tag{2}$$

$$\rho\left(\frac{\partial v_z}{\partial t}+v_r\frac{\partial v_z}{\partial r}+v_z\frac{\partial v_z}{\partial z}\right)=-\frac{\partial P}{\partial z}+\mu\left[\frac{1}{r}\frac{\partial}{\partial r}\left(r\frac{\partial v_z}{\partial r}\right)+\frac{1}{r_2}\frac{\partial^2 v_z}{\partial\theta^2}+\frac{\partial^2 v_z}{\partial z^2}\right] \tag{3}$$

In order to compare the order of magnitude of each term of Eqs. (1) to (3), one may make these equations dimensionless.

For the characteristic pressure of fan-shaped geometry (Fig. 1),

the force balance between r=R′ (randomly chosen between r=R_1 and r=R_0) and r=R_0, can be approximated as below.

$$\hat{\theta}(R'hP'-R_0hP_0)=\frac{\hat{\theta}}{2}(R_0^2-R'^2)\mu\frac{\bar{v}_r}{h} \tag{4}$$

where $\hat{\theta}$ is the vertex angle of the fanshaped radial flow and $\bar{v}_r$ is not only average velocity between r=R′ and r=R_0 but also characteristic velocity in r direction.

In Fig. 1, P_0 corresponds to the pressure of gas phase between leading melt phase front and the end of the mold with appropriate vent area in gas assisted injection molding and is assumed to be negligible compared to P′ so that P′≫(R_0/R′) P_0.

Thus Eq. (4) can be reduced into:

$$\hat{\theta}R'hP'=\frac{\hat{\theta}}{2}(R_0^2-R'^2)\mu\frac{\bar{v}_r}{h} \tag{5}$$

Setting R′ as R_0/2, P′ becomes $3\mu\bar{v}_r R_0/4h^2$ which is $3\mu\bar{v}_r R_0/H^2$. Thus the characteristic pressure, $\bar{P}$, may be set as $\mu\bar{v}_r R_0/H^2$ to render di- mensionless pressure, $\tilde{P}$, into P/$\bar{P}$ in this manner.

Further dimensionless variables are taken as:

$$\tilde{v}_r=\frac{v_r}{\bar{v}_r},\tilde{v}_z=\frac{v_z}{\bar{v}_z},\tilde{r}=\frac{r}{R_0},\tilde{z}=\frac{z}{H},\tilde{\theta}=\frac{\theta}{\hat{\theta}}\text{ and }\tilde{t}=\frac{t}{\hat{t}}$$

where $\hat{t}$ is chosen as $R_0/\bar{v}_r$ and $\bar{v}_z$ is chosen as $H/R_0\bar{v}_r$.

Then continuity and momentum equations are rendered into dimensionless form as below.

$$\frac{1}{\tilde{r}}\frac{\partial}{\partial\tilde{r}}(\tilde{r}\tilde{v}_r)+\frac{\partial\tilde{v}_z}{\partial\tilde{z}}=0 \tag{6}$$

$$\frac{\rho\bar{v}_rH}{\mu}\left(\frac{H}{R_0}\right)\left[\frac{\partial\tilde{v}_r}{\partial\tilde{t}}+\tilde{v}_r\frac{\partial\tilde{v}_r}{\partial\tilde{r}}+\tilde{v}_z\frac{\partial\tilde{v}_r}{\partial\tilde{z}}\right]$$
$$=-\frac{\partial\tilde{P}}{\partial\tilde{r}}+\frac{\partial^2\tilde{v}_r}{\partial\tilde{z}^2}+\left(\frac{H}{R_0}\right)^2\left(\frac{\partial}{\partial\tilde{r}}\left(\frac{1}{\tilde{r}}\frac{\partial}{\partial\tilde{r}}(\tilde{r}\tilde{v}_r)\right)\right)+\left(\frac{H}{R_0}\right)^2\frac{1}{\hat{\theta}^2}\left(\frac{1}{\tilde{r}^2}\frac{\partial^2\tilde{v}_r}{\partial\tilde{\theta}^2}\right) \tag{7}$$

$$\frac{\rho\bar{v}_rH}{\mu}\left(\frac{H}{R_0}\right)^3\left[\frac{\partial\tilde{v}_z}{\partial\tilde{t}}+\tilde{v}_r\frac{\partial\tilde{v}_z}{\partial\tilde{r}}+\tilde{v}_z\frac{\partial\tilde{v}_z}{\partial\tilde{z}}\right]$$
$$=-\frac{\partial\tilde{P}}{\partial\tilde{z}}+\left[\left(\frac{H}{R_0}\right)^4\left\{\frac{1}{\tilde{r}}\frac{\partial}{\partial\tilde{r}}\left(\tilde{r}\frac{\partial\tilde{v}_z}{\partial\tilde{r}}\right)+\frac{1}{\hat{\theta}^2}\frac{1}{\tilde{r}^2}\frac{\partial^2\tilde{v}_z}{\partial\hat{\theta}^2}\right\}+\left(\frac{H}{R_0}\right)^2\frac{\partial^2\tilde{v}_z}{\partial\tilde{z}^2}\right] \tag{8}$$

When $(H/R_0)^2 1/\hat{\theta}^2 \ll 1$ and $(H/R_0)^2$ is the same order as or less than 0 (1), neglecting end effects on both sides in θ direction, the behavior of the flow between two fan-shaped plates in conventional injection molding may be considered as the part (i.e., $\hat{\theta}/2\pi$) of the radial flow between two entire round plates. When $\rho\bar{v}_r H/\mu(H/R_0) \ll 1$, $(H/R_0)^2 1/\hat{\theta}^2 \ll 1$ and $(H/R_0)^2 \ll 1$ the flow model of Newtonian fluid was previously suggested under the fan-shaped geometry [Lim, 1999, 2004a].

On the other hand for $\rho\bar{v}_r H/\mu(H/R_0) \ll (H/R_0)^2 \ll 1$ $(H/R_0)^2$ and $(H/R_0)^2 1/\hat{\theta}^2$ may be replaced by small parameter, ε when $\hat{\theta}^2$ is the order of one. Hence Eqs. (7) and (8) may be reduced into quasi-steady state equations as:

$$0=-\frac{\partial\tilde{P}}{\partial\tilde{r}}+\frac{\partial^2\tilde{v}_r}{\partial\tilde{z}^2}+\varepsilon\left(\frac{\partial}{\partial\tilde{r}}\left(\frac{1}{\tilde{r}}\frac{\partial}{\partial\tilde{r}}(\tilde{r}\tilde{v}_r)\right)+\frac{1}{\tilde{r}^2}\frac{\partial^2\tilde{v}_r}{\partial\tilde{\theta}^2}\right)+0(\varepsilon^2) \tag{9}$$

$$0=-\frac{\partial\tilde{P}}{\partial\tilde{z}}+\varepsilon\frac{\partial^2\tilde{v}_z}{\partial\tilde{z}^2}+0(\varepsilon^2) \tag{10}$$

In addition $\tilde{P}$, $\tilde{v}_r$, and $\tilde{v}_z$ may be perturbed around $(\tilde{P})_0$, $\tilde{v}_{r0}$, and $\tilde{v}_{z0}$, using perturbation technique, in terms of ε as:

$$\tilde{P}=(\tilde{P})_0+(\tilde{P})_1\varepsilon+0(\varepsilon^2) \tag{11}$$

$$\tilde{v}_r=\tilde{v}_{r0}+\tilde{v}_{r1}\varepsilon+0(\varepsilon^2) \tag{12}$$

$$\tilde{v}_z=\tilde{v}_{z0}+\tilde{v}_{z1}\varepsilon+0(\varepsilon^2) \tag{13}$$

Eqs. (11) to (13) may be substituted into Eqs. (9) and (10). Then those equations and their boundary conditions at both $\tilde{z}=0.5$ and $\tilde{z}=-0.5$, may be sorted in accordance with the order of magnitude of each term of two equations.

1) 0(1):

$$0=-\frac{\partial(\tilde{P})_0}{\partial\tilde{r}}+\frac{\partial^2\tilde{v}_{r0}}{\partial\tilde{z}^2} \tag{14}$$

$$0=-\frac{\partial(\tilde{P})_0}{\partial\tilde{z}} \tag{15}$$

B.C.: $\tilde{v}_{r0}(\tilde{z}=\pm0.5)=0$

2) 0(ε):

$$0=-\frac{\partial(\tilde{P})_1}{\partial\tilde{r}}+\frac{\partial^2\tilde{v}_{r1}}{\partial\tilde{z}^2}+\frac{\partial}{\partial\tilde{r}}\left(\frac{1}{\tilde{r}}\frac{\partial}{\partial\tilde{r}}(\tilde{r}\tilde{v}_{r0})\right)+\frac{1}{\tilde{r}^2}\frac{\partial^2\tilde{v}_{r0}}{\partial\tilde{\theta}^2} \tag{16}$$

$$0=-\frac{\partial(\tilde{P})_1}{\partial\tilde{z}}+\frac{\partial^2\tilde{v}_{z0}}{\partial\tilde{z}^2} \tag{17}$$

B.C.: $\tilde{v}_{r1}(\tilde{z}=\pm0.5)=0$

With appropriate procedures the solutions of Eqs. (14) and (15) may be derived, as previously derived in Lim [1999, 2004a], as below:

$$\tilde{v}_{r0}(\tilde{r},\tilde{z})=\frac{1}{2\tilde{r}}\frac{(\tilde{P}_1)_0-(\tilde{P}_0)_0}{\ln\frac{R_1}{R_0}}\left(\tilde{z}^2-\frac{1}{4}\right) \tag{18}$$

$$\tilde{v}_{z0}(\tilde{r},\tilde{z})=0 \tag{19}$$

Then the pressure distribution of 0(1) becomes

$$(\tilde{P})_0=\frac{(\tilde{P}_1)_0-(\tilde{P}_0)_0}{\ln\frac{R_1}{R_0}}\ln\tilde{r}+(\tilde{P}_0)_0 \tag{20}$$

Substituting Eqs. (18) and (19) into Eq. (16) and (17), respectively, one may obtain a similar set of P. D. E.s for 0(ε) to that for 0(1) as below:

$$0=-\frac{\partial(\tilde{P})_1}{\partial\tilde{r}}+\frac{\partial^2\tilde{v}_{r1}}{\partial\tilde{z}^2} \tag{21}$$

$$0=-\frac{\partial(\tilde{P})_1}{\partial\tilde{z}} \tag{22}$$

B.C.: $\tilde{v}_{r1}(\tilde{z}=\pm0.5)=0$

Thus the solutions for 0(ε) becomes:

$$\tilde{v}_{r1}(\tilde{r},\tilde{z})=\frac{1}{2\tilde{r}}\frac{(\tilde{P}_1)_1-(\tilde{P}_0)_1}{\ln\frac{R_1}{R_0}}\left(\tilde{z}^2-\frac{1}{4}\right) \tag{23a}$$

$$\tilde{v}_{z1}(\tilde{r},\tilde{z})=0 \tag{23b}$$

Then the pressure distribution of 0(ε) becomes

$$(\tilde{P})_1=\frac{(\tilde{P}_1)_1-(\tilde{P}_0)_1}{\ln\frac{R_1}{R_0}}\ln\tilde{r}+(\tilde{P}_0)_1 \tag{24}$$

Consequently, one may obtain the following solutions truncating the terms less than or equal to $0(\varepsilon^2)$:

$$\tilde{v}_r(\tilde{r},\tilde{z}) = \frac{1}{2\tilde{r}}\frac{\tilde{P}_1-\tilde{P}_0}{\ln\frac{R_1}{R_0}}\left(\tilde{z}^2-\frac{1}{4}\right)+0(\varepsilon^2) \tag{25}$$

$$\tilde{v}_z(\tilde{r},\tilde{z}) = 0(\varepsilon^2) \tag{26}$$

$$\tilde{P} = \frac{\tilde{P}_1-\tilde{P}_0}{\ln\frac{R_1}{R_0}}\ln\tilde{r}+\tilde{P}_0+0(\varepsilon^2) \tag{27a}$$

when $\rho\bar{v}_r H/\mu(H/R_0)<<(H/R_0)^2<<1$ and $\hat{\theta}^2$ is 0(1).

Thus the pressure distribution may be first order-approximated, neglecting $0(\varepsilon^2)$ from Eq. (27a), as:

$$P = \frac{P_1-P_0}{\ln\frac{R_1}{R_0}}\ln\frac{r}{R_0}+P_0 \tag{27b}$$

where P_1 and P_0 is the pressure at $r=R_1$ and R_0 respectively.

The velocity profile may be also approximated up to first order as:

$$v_r(r,z) = \frac{h^2}{2\mu r}\frac{P_1-P_0}{\ln\frac{R_1}{R_0}}\left(\frac{z^2}{h^2}-1\right) \tag{28}$$

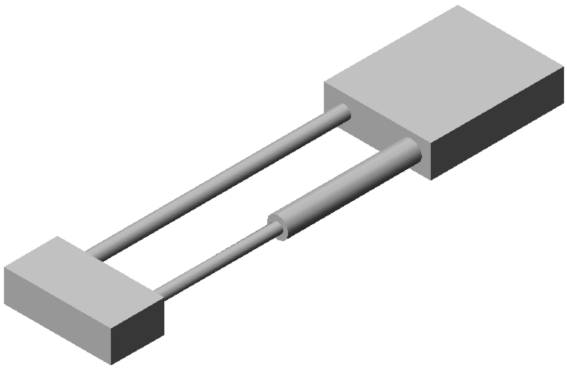

Fig. 2a. A cavity composed of two pipes, pipe 1 and pipe 2, connected in parallel. Thick cavities of two square flat plates (SFP) are attached to each side of these pipes. The length, depth and width of a cavity between two SFP were 20 mm, 12 mm and 40 mm, respectively.

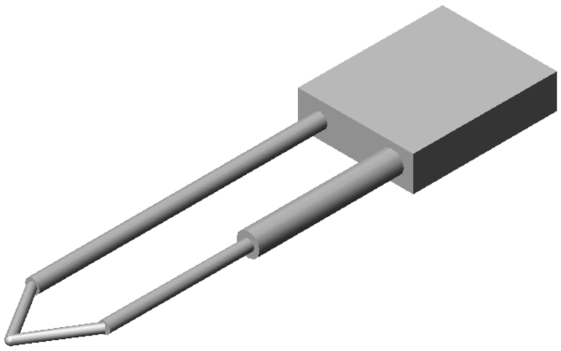

Fig. 2b. A cavity composed of two pipes, pipe 1 and pipe 2, connected in parallel. At the left side of these pipes branching runners are replaced for a thick cavity of two square plates to deliver resin to both sides of pipes.

when $\rho\bar{v}_r H/\mu(H/R_0)<<(H/R_0)^2<<1$ and $\hat{\theta}^2$ is 0(1).

Integrating $v_r(r, z)$ from Eq. (28) with z, the expression of melt phase flow rate (Q) of Eq. (29) is obtained as:

$$Q = \hat{\theta}rH\langle v_r\rangle = 2\int_0^h v_r(r,z)\hat{\theta}rdz = \frac{2\hat{\theta}h^3}{3\mu}\frac{P_1-P_0}{\ln\frac{R_0}{R_1}} \tag{29}$$

where $\langle v_r\rangle$: average velocity of melt phase flow

Eq. (29) may be rearranged as:

$$\Delta P_{fan\text{-}plates} = \frac{12\mu Q}{H^3\hat{\theta}}\ln\frac{R_0}{R_1} = \frac{12\mu r\langle V_r\rangle}{H^2}\ln\frac{R_0}{R_1} \tag{30}$$

when $\rho\bar{v}_r H/\mu(H/R_0)<<(H/R_0)^2<<1$ and $\hat{\theta}^2$ is 0(1).

One may frequently encounter the problem of fan-shaped cavity between two square plates where $(H/R_0)^2$ is around 10^{-1} instead of the limiting condition of $(H/R_0)^2<<1$, and $\hat{\theta}^2$ is the order of one.

Eqs. (28), (29) and (30) may be eligible without significant error to the problem of fan-shaped geometry in case that not only $(H/R_0)^2 \ll 1$ but also $(H/R_0)^2$ is even around 10^{-1} with the condition of $\rho\bar{v}_r H/\mu(H/R_0)<<(H/R_0)^2$.

2. Resistance of Heterogeneous Geometries

Figs. 2a and 2b show a cavity composed of two pipes, pipe 1 and pipe 2, connected in parallel. Relatively thick cavities of two square plates are attached to each side of these pipes in Fig. 2a. The left-relatively thick cavity of two square plates is replaced by two runners as in Fig. 2b. Pipe 1 is composed of pipe 11 and pipe 12 connected in series, and pipe 2 is composed of pipe 21 and pipe 22. These four pipes have the same length and may or may not have the same diameter. The polymer and gas injection points are located at the center of the front side of a relatively thick cavity between two square plates in the left hand side. Pipe 1 is located at the upper side and pipe 2 is at the lower side. In this paper subscript 11 and subscript 12 denote the first pipe and the second pipe from the left hand side at the upper side respectively while subscript 21 and subscript 22 denote the first pipe and the second pipe from the left hand side at the lower side, respectively.

2-1. Definition of Proposed Resistance

The definition of resistance may be developed and proposed to be r^* as a resistance to V^* of the initial velocity of melt polymer at the nearest geometry to a gas injection point, while the resistance to flow rate was previously defined as r [Lim and Lee, 2003]. Consequently, the proposed resistance of steady state flow of a Newtonian liquid under the following geometry may be rearranged as below.

2-2. Proposed Resistance for Four Conduits

$$\Delta p_1 = Q_1 r_1 = V^* r_1^* = V_{11} r_1^* \tag{31}$$

$$\Delta p_2 = Q_2 r_2 = V^* r_2^* = V_{21} r_2^* \tag{32}$$

where

$$r_1^* = \frac{\pi}{4}D_{11}^2 r_1 = 32\mu D_{11}^2\left(\frac{L_{11}}{D_{11}^4}+\frac{L_{12}}{D_{12}^4}\right) \tag{33}$$

$$r_2^* = \frac{\pi}{4}D_{21}^2 r_2 = 32\mu D_{21}^2\left(\frac{L_{21}}{D_{21}^4}+\frac{L_{22}}{D_{22}^4}\right) \tag{34}$$

Thus

$$\frac{r_2^*}{r_1^*} = \frac{r_2 D_{21}^2}{r_1 D_{11}^2} \tag{35}$$

2-3. Proposed Resistance for the Cavity between Two SFP

Eq. (30) may be transformed into the form that includes the velocity (V^*) instead of the flow rate (Q), at the half of the distance of initial leading melt front. Then the proposed resistance of steady state flow of a Newtonian liquid under fan-shaped geometry may be rearranged as below.

$$\Delta P = V^* r^* \text{ where } r^* = \frac{12\mu}{H^2}\frac{R_0}{2}\ln\frac{R_0}{R_1} \tag{36}$$

if $\rho \bar{v}_r H/\mu(H/R_0)<<(H/R_0)^2<<1$ and $\hat{\theta}^2$ is 0(1).

2-4. Proposed Rule of Thumb under the Geometry Composed of a Cavity between Two SFP and Four Conduits

One may consider that the vertex angle of fan-shaped path (i.e., $\hat{\theta}$) for gas penetration may be divided into two sections for both the upper and the lower sides. For each side the vertex angle may become $\hat{\theta}/2$. The flow rate (Q_1) for the upper side may be described with the initial velocity of melt resin at the half of the distance of initial leading melt front as:

$$Q_1 = \left(\frac{R_0}{2}\right)\left(\frac{\hat{\theta}}{2}\right) H V_1^*\left(r = \frac{R_0}{2}\right) \tag{37}$$

The pressure drop under the combined geometries may be expressed for the upper side as:

$$\Delta P = V_1^* r_1^* \tag{38}$$

where , $r_1^* = \left(\frac{R_0}{2}\right)\left(\frac{\hat{\theta}}{2}\right) H\left[\frac{12\mu}{H^3\frac{\hat{\theta}}{2}}\ln\frac{R_0}{R_1} + \frac{128\mu}{\pi}\left(\frac{L_{11}}{D_{11}^4} + \frac{L_{12}}{D_{12}^4}\right)\right]$,

if $\rho \bar{v}_r H/\mu(H/R_0)<<(H/R_0)^2<<1$ and $\hat{\theta}^2$ is 0(1).

In the same manner the pressure drop may be described for the lower side of the configuration.

Thus

$$\frac{V_1^*}{V_2^*} = \frac{r_2^*}{r_1^*} \tag{39}$$

where

$$r_1^* = \left(\frac{R_0}{2}\right)\left(\frac{\hat{\theta}}{2}\right) H\left[\frac{12\mu}{H^3\frac{\hat{\theta}}{2}}\ln\frac{R_0}{R_1} + \frac{128\mu}{\pi}\left(\frac{L_{11}}{D_{11}^4} + \frac{L_{12}}{D_{12}^4}\right)\right] \tag{40}$$

$$r_2^* = \left(\frac{R_0}{2}\right)\left(\frac{\hat{\theta}}{2}\right) H\left[\frac{12\mu}{H^3\frac{\hat{\theta}}{2}}\ln\frac{R_0}{R_1} + \frac{128\mu}{\pi}\left(\frac{L_{21}}{D_{21}^4} + \frac{L_{22}}{D_{22}^4}\right)\right] \tag{41}$$

Table 1. Simulation conditions of MOLDFLOW

Simulation factor	Description
Resin filling	Short shot molding (85-95%)
Gas control	Volume control
Resin	PET (DP400)
Resin melt temperature	210 °C
Mold temperature	100 °C
Gas injection pressure	15 M pascal
Gas delay time	0.5 sec
Gas piston time	1 sec

3. Simulations and Model-predictions

The simulation and model-prediction were performed under the geometry composed of two pipes (pipe 1 and pipe 2) connected in parallel as well as two relatively thick cavities between two square-flat-plates (SFP) attached to each side of them as shown in Fig. 2a. The initial polymer shut-off totally filled the cavities of a pipe 1 and pipe 2 (center) as well as the left (polymer/gas nozzle side) cavity between two SFP. On the other hand the right cavity between two SFP was partially filled by 85-90% with melt resin due to a short shot. The length, depth and width of a cavity between two SFP were

Table 2. Various geometrical conditions of pipes as in Fig. 2a

Case	D_1	D_{21}	D_{22}
Fig. 3	5 mm	6 mm	4 mm
Fig. 4	5 mm	8 mm	4 mm
Fig. 5	5 mm	10 mm	4 mm
Fig. 6	5 mm	2 mm	8 mm
Fig. 7	5 mm	4 mm	8 mm
Fig. 8	5 mm	5 mm	4.5 mm
Fig. 9	4.5 mm	5 mm	4.5 mm
Fig. 10	4.5 mm	7.5 mm	5 mm
Fig. 11	6 mm	5.5 mm	6 mm

Table 3. Various geometrical conditions of runners and pipes as in Fig. 2b

Case	D_1'	D_2'	D_1	D_{21}	D_{22}
Fig. 12	3 mm	3 mm	5 mm	8 mm	4 mm
Fig. 13	3 mm	3 mm	5 mm	10 mm	4 mm
Fig. 14	3 mm	3 mm	5 mm	2 mm	8 mm
Fig. 15	3 mm	3 mm	5 mm	4 mm	8 mm
Fig. 16	3 mm	3 mm	5 mm	4.2 mm	8 mm
Fig. 17	3 mm	3 mm	5 mm	7 mm	4.5 mm
Fig. 18	3 mm	3 mm	5 mm	8 mm	4.5 mm
Fig. 19	3 mm	3 mm	5 mm	9 mm	4.5 mm

Table 4. Values of dimensionless numbers

D (mm)	L (mm)	$\bar{v}_r$ (m/s)	$\frac{\rho \bar{v}_r H}{\mu}\left(\frac{H}{R_0}\right)$	$\left(\frac{H}{R_0}\right)^2 \frac{1}{\left(\frac{\hat{\theta}}{2}\right)^2}$
2	100	0.0039	0.00010	0.14605
3	100	0.0198	0.00053	0.14605
4	100	0.0624	0.00166	0.14605
5	100	0.15169	0.00404	0.14605
6	100	0.31225	0.00833	0.14605
7	100	0.57164	0.01524	0.14605
8	100	0.95783	0.02554	0.14605
9	100	1.49551	0.03988	0.14605
10	100	2.20184	0.05872	0.14605

• The values of R_1, R_0, H and $\hat{\theta}$ were given as 1 mm, 20 mm, 12 mm and π, respectively.

• Each value of $\bar{v}_r$ at $r'=R_0/2$ was calculated from Eq. (38) where viscosity of 270 Pa sec was assumed.

20 mm, 12 mm and 40 mm, respectively. Pipe 1 and pipe 2 were composed of two identical or different pipes, respectively, each of which was 50 mm long. Both ends of pipe 1 and pipe 2 were connected to the left and right cavities between two SFP, respectively. The connection points between pipes and the cavities between two SFP were located at the centers of the 1st and 2nd half of the cavity-width. The vertex angle ($\hat{\theta}$) of fan-shaped cavity was initially π and it remained at this value at the incipient stage of gas penetration. Thus the value of vertex angle ($\hat{\theta}$) was chosen π to apply to the proposed rule of thumb or flow model. In addition, simulation and model-prediction were performed under the geometry composed of two pipes (pipe 1 and pipe 2) connected in parallel as well as a runner and a relatively thick cavity attached to L. H. S. and R. H. S. of them, respectively, as shown in Fig. 2b. The simulation conditions were as the same as given in Table 1 when the commercial software of MOLDFLOW (version of MPI 4.1) was used to perform the simulations of the cases as shown in Tables 2 and 3. Tables 2 and 3 show geometrical conditions situated when the cavities of pipes (center) as well as two cavities between two SFP (left and right) and the cavities of pipes (center), a runner as well as a cavity between two SFP (right) were involved in the configuration as in Fig. 2a and Fig. 2b, respectively. The diameter of each pipe varied from 2 mm to 10 mm as in Tables 2 and 3. For each case of Tables 2 and 3 the volume ratio of resin filling at polymer shut-off was chosen between 85%-95% to avoid blow-through at the stage of gas injection. Table 4 shows the values of dimensionless numbers for various values of diameter of pipe (L=100 mm) attached to the cavity of two SFPs, of which the criterion met the condition that $(H/R_0)^2 1/(\hat{\theta}/2)^2$ and $(H/R_0)^2$ are around 10^{-1} with the condition that $\rho \bar{v}_r H/\mu (H/R_0) \ll (H/R_0)^2$ to satisfy Eq. (38) even though the small pameter, ε, became larger.

Finite element method (FEM) was adopted to simulate the center (a pipe) and the left and right hand sides (SFP), modeled with line-elements and triangle-elements respectively, of Fig. 2a in the environment of MOLDFLOW (version of MPI 4.1). In the similar manner, as in Fig. 2b, finite element method (FEM) was adopted to simulate the center (a pipe), the left (runner) and the right hand side (SFP), modeled with line-elements, line elements and triangle-elements, respectively.

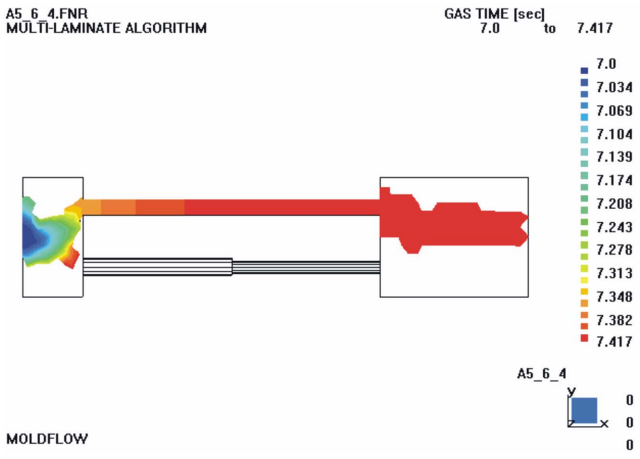

Fig. 3. Pipe 11 with a diameter of 5 mm and a length of 50 mm is connected to pipe 12 with a diameter of 5 mm and a length of 50 mm. Pipe 21 with a diameter of 6 mm and a length of 50 mm is connected in series with pipe 22 with a diameter of 4 mm and a length of 50 mm.

Table 5. Comparison of simulation results and proposed rule of thumbs (RT1 and RT2)

Case	RT1	RT2	Flow direction (Simulation results)
Fig. 3	1.46 (○)	2.11 (○)	Upper
Fig. 4	1.30 (○)	3.32 (○)	Upper
Fig. 5	1.25 (○)	5.01 (○)	Upper
Fig. 6	19.57 (○)	3.13 (○)	Upper
Fig. 7	1.29 (×)	0.83 (○)	Lower
Fig. 8	1.26 (○)	1.26 (○)	Upper
Fig. 9	0.83 (○)	1.02^c (×)	Lower
Fig. 10	0.39 (○)	1.09^c (×)	Lower
Fig. 11	1.21 (○)	1.02^c (○)	Upper

- RT1 and RT2 are the results of the proposed rules of thumb from Eqs. (39) and (35), respectively.
- The values of R_0, R_1 and H were given as 1 mm, 20 mm and 12 mm respectively.
- "○" and "×" denotes "correct" and "incorrect" respectively.
- The superscript of c in Table 5 denotes that its ratio of resistances is very close to unity.

RESULTS AND DISCUSSION

1. Situation when Cavities of Pipes and Thick Plates are Involved in the Configuration

As in Fig. 2a, at the upper side, pipe 11 with the length of 50 mm was connected to pipe 12 with the same diameter and the same length as pipe 11. At lower side, pipe 21 with the length of 50 mm was connected in series to pipe 22 with the same length of 50 mm. The applied diameters of pipes are shown in Table 2. Consider a situation where a resin fluid is flowing to the direction of right hand side at steady state. For Figs. 3 to 10, the rule of thumb of Eq. (39) was utilized to obtain the value of ratio (RT1) of initial resin radial veloc-

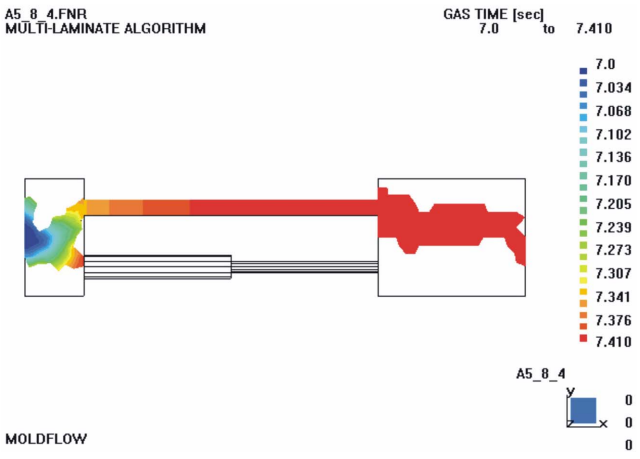

Fig. 4. The geometry is the same as Fig. 3 except that diameter of pipe 21 is 8 mm.

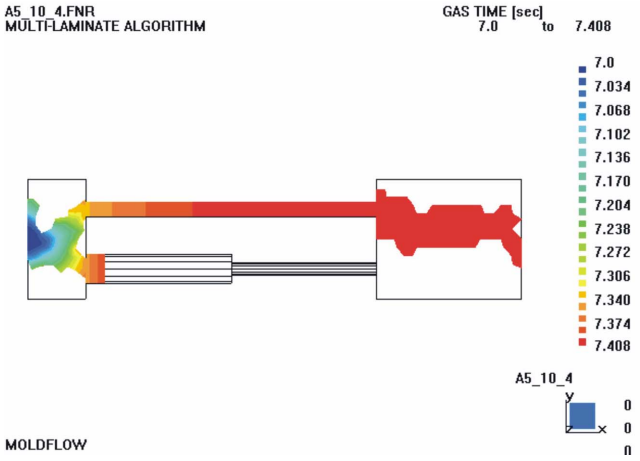

Fig. 5. The geometry is the same as Fig. 3 except that diameter of pipe 21 is 10 mm.

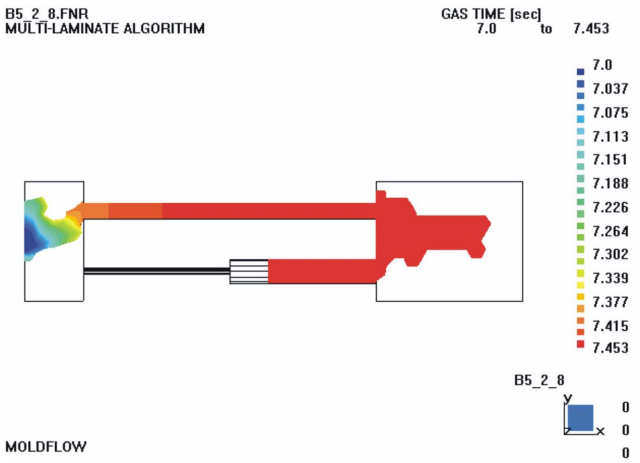

Fig. 6. Pipe 11 with a diameter of 5 mm and a length of 50 mm is connected to pipe 12 with a diameter of 5 mm and a length of 50 mm. Pipe 21 with a diameter of 2 mm and a length of 50 mm is connected in series with pipe 22 with a diameter of 8 mm and a length of 50 mm.

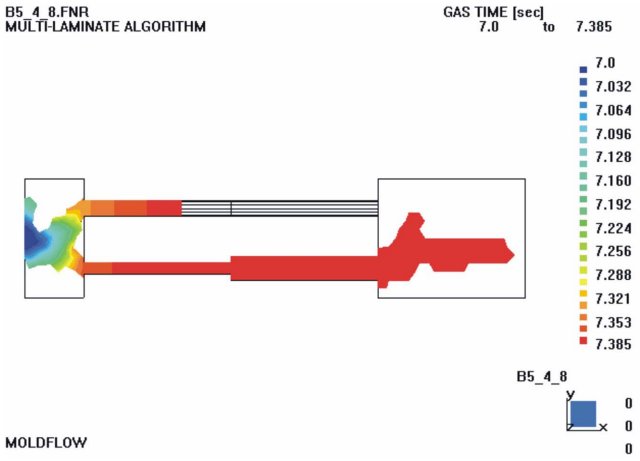

Fig. 7. The geometry is the same as Fig. 6 except that diameter of pipe 21 is 4 mm.

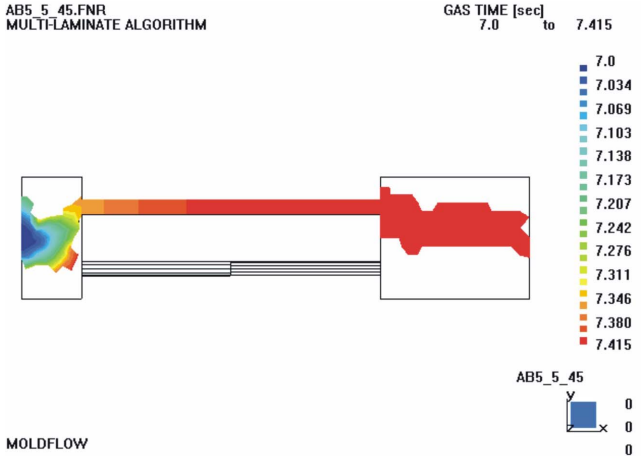

Fig. 8. Pipe 11 with a diameter of 5 mm and a length of 50 mm is connected to pipe 12 with a diameter of 5 mm and a length of 50 mm. Pipe 21 with a diameter of 5 mm and a length of 50 mm is connected in series with pipe 22 with a diameter of 4.5 mm and a length of 50 mm.

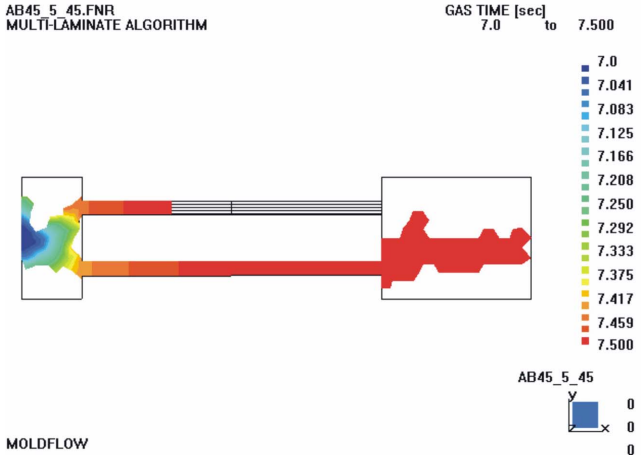

Fig. 9. The geometry is the same as Fig. 8 except that diameter of pipe 1 is 4.5 mm.

ities at $r=R_0/2$ for upper side and lower side of the configuration. Similarly, the rule of thumb of Eq. (35) was used to evaluate the vale of the ratio of initial axial velocity as RT2. Thus RT1 may be used as a criterion to determine where the gas flows earlier between to upper pipes and to lower pipes while RT2 may be used to determine where the gas flows faster between inside upper pipes and inside lower pipes. Table 5 provides the values of RT1 and RT2 for Figs. 3 to 11. The results of simulations were generally consistent with the former, except for Fig. 7, in a qualitative way to determine gas directions in gas assisted injection molding even though a relatively large value of 0.36 was applied as the value of ε to describe a relatively thick cavity of two square plates. One may observe that the gas flows somewhat faster or slower in the upper side of the cavity of two SFP than in the lower side for Figs. 3, 4, 5, 8 and 11 or Figs. 9 and 10, respectively, where the values of RT1 are near 1.0. However, the gas direction was initially determined to upper side as in Fig. 6 where the gas flows drastically faster in the upper side since the value of RT1 becomes 19.57. Yet, it may be observed

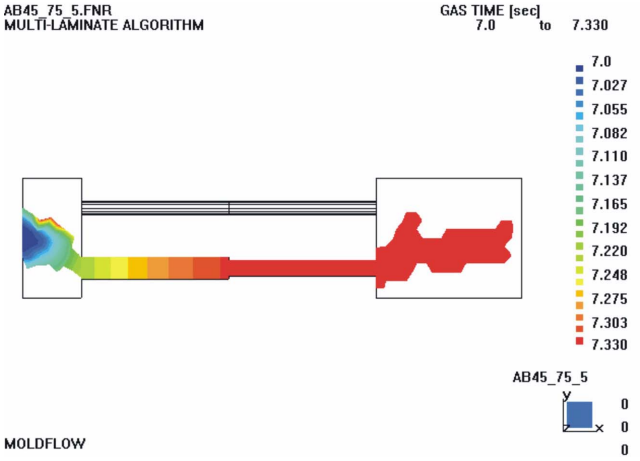

Fig. 10. Pipe 11 with a diameter of 4.5 mm and a length of 50 mm is connected to pipe 12 with a diameter of 4.5 mm and a length of 50 mm. Pipe 21 with a diameter of 7.5 mm and a length of 50 mm is connected in series with pipe 22 with a diameter of 5 mm and a length of 50 mm.

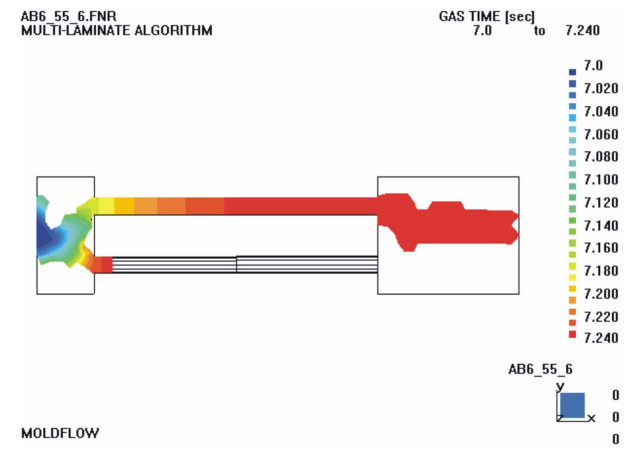

Fig. 11. Pipe 11 with a diameter of 6 mm and a length of 50 mm is connected to pipe 12 with a diameter of 6 mm and a length of 50 mm. Pipe 21 with a diameter of 5.5 mm and a length of 50 mm is connected in series with pipe 22 with a diameter of 6 mm and a length of 50 mm.

that the gas flows somewhat faster or slower in the upper pipe 1 than in the lower pipe 21 for Figs. 3, 4, 5, 6, 8 and 11 or Fig. 7, respectively, which is consistent with flow directions predicted according to the values of RT2 as in Table 5. For exceptional cases, RT1 was not consistent with the simulation results (i.e., flow directions) in the case of Fig. 7 while RT2 was not consistent in the cases of Figs. 9 and 10. This may be generally interpreted, for Fig. 7, as that the gas may not flow to pipes of the side where the gas enters earlier if the gas flows slower in the pipes of that side; and for Figs. 9 and 10, as that the gas may flow to pipes of the side where the gas enters earlier even if the gas flows a little bit slower in those pipes. Thus, such a developed model as time-dependent model is required to describe transient behavior of the interface between gas phase and resin phase, which will be treated in part 2 of this paper.

2. Situation when Cavities of Pipes and Runners are Involved

Table 6. Comparison of simulation results and proposed rules of thumb

Case	RT	CRT	Flow direction (Simulation results)
Fig. 12	1.06^c (○)	2.71 (○)	Upper
Fig. 13	1.05^c (○)	4.20 (○)	Upper
Fig. 14	4.77 (○)	N/A	Upper
Fig. 15	1.06^c (×)	0.68 (○)	Lower
Fig. 16	1.01^c (×)	0.72 (○)	Lower
Fig. 17	0.98^c (×)	1.92 (○)	Upper
Fig. 18	0.97^c (×)	2.48 (○)	Upper
Fig. 19	0.96^c (×)	3.12 (○)	Upper

• RT and CRT are the results of the modified rules of thumb from Eq. (35) to include the effect of runners and its corrected rule of thumb, respectively.
• "○" and "×" denotes "correct" and "incorrect", respectively.
• The superscript of c in Table 6 denotes that its ratio of resistances is very close to unity.

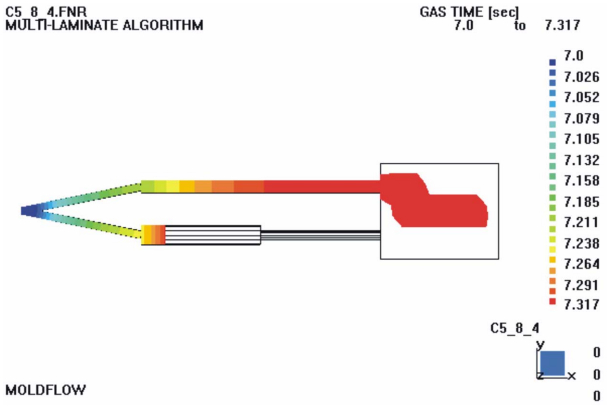

Fig. 12. The geometry is similar to Fig. 4. Instead of a thick cavity of two square plates, branching runners with diameter of 3 mm are attached at the left hand side to deliver resin to pipes at both upper side and lower side.

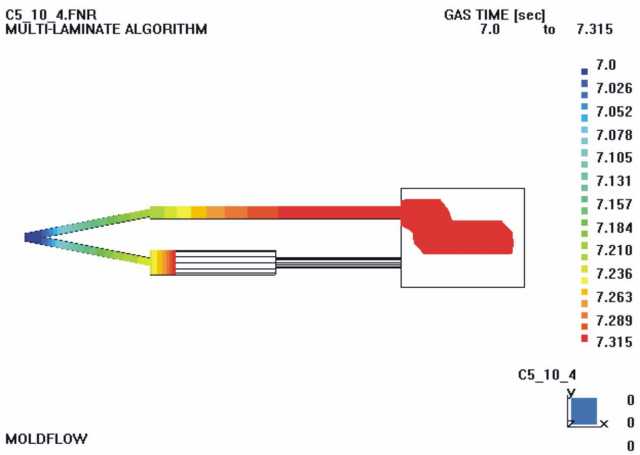

Fig. 13. The geometry is similar to Fig. 5. Instead of a thick cavity of two square plates, branching runners with diameter of 3 mm are attached at the left hand side to deliver resin to pipes at both upper side and lower side.

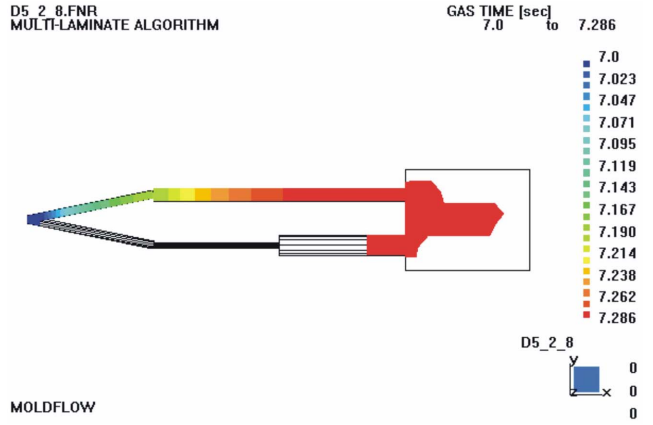

Fig. 14. The geometry is similar to Fig. 6. Instead of a thick cavity of two square plates, branching runners with diameter of 3 mm are attached at the left hand side to deliver resin to pipes at both upper side and lower side.

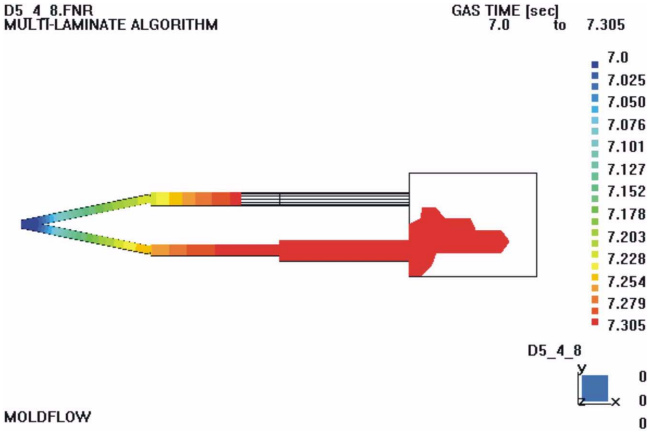

Fig. 15. The geometry is similar to Fig. 7. Instead of a thick cavity of two square plates, branching runners with diameter of 3 mm are attached at the left hand side to deliver resin to pipes at both upper side and lower side.

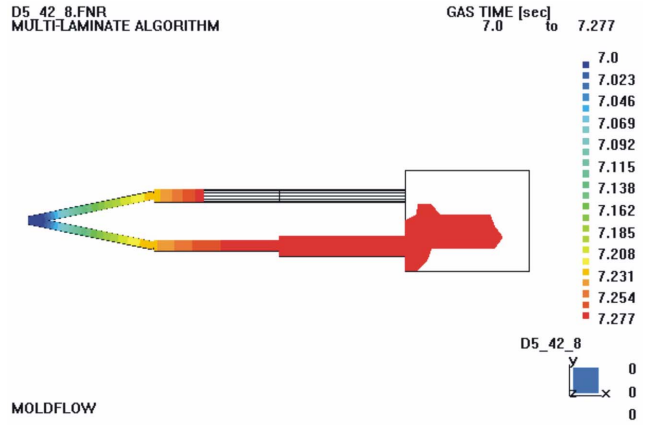

Fig. 16. The geometry is similar to Fig. 7 except that diameter of pipe 21 is 4.2 mm. Instead of a thick cavity of two square plates, branching runners with diameter of 3 mm are attached at the left hand side to deliver resin to pipes at both upper side and lower side.

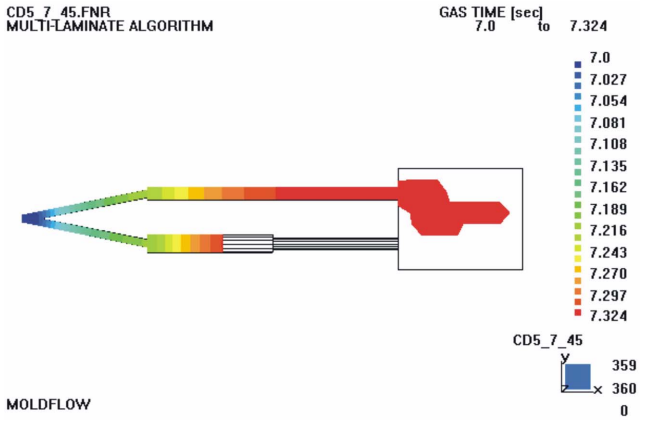

Fig. 17. The geometry is similar to Fig. 8 except that diameter of pipe 21 is 7 mm. Instead of a thick cavity of two square plates, branching runners with diameter of 3 mm are attached at the left hand side to deliver resin to pipes at both upper side and lower side.

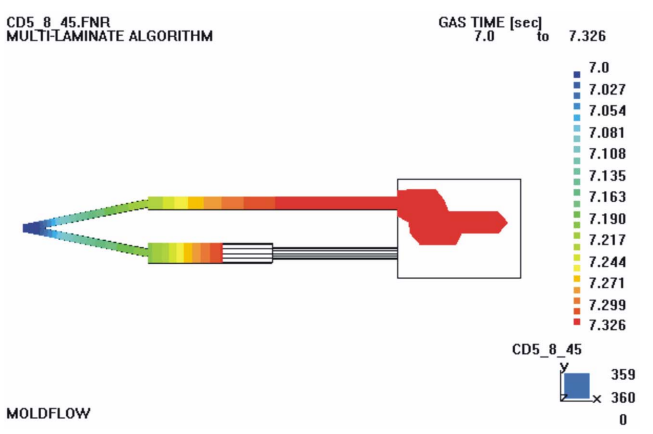

Fig. 18. The geometry is similar to Fig. 8 except that diameter of pipe 21 is 8 mm. Instead of a thick cavity of two square plates, branching runners with diameter of 3 mm are attached at the left hand side to deliver resin to pipes at both upper side and lower side.

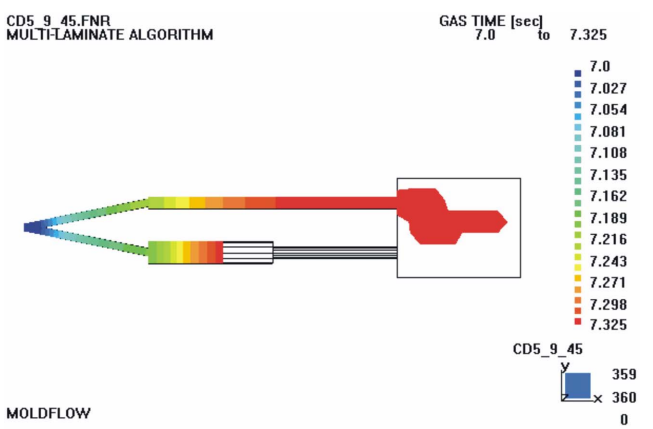

Fig. 19. The geometry is similar to Fig. 8 except that diameter of pipe 21 is 9 mm. Instead of a thick cavity of two square plates, branching runners with diameter of 3 mm are attached at the left hand side to deliver resin to pipes at both upper side and lower side.

in Configuration

Fig. 2b shows a cavity composed of two pipes, pipe 1 and pipe 2, connected in parallel. At the left side of these pipes a thick cavity of two square plates is replaced with branching runners to deliver resin to both sides of pipes. The length (L_1') and the diameter (D_1') of the runners at the upper side of pipes are 51 mm and 3 mm, respectively. The same geometric condition is applied to the runner at the lower side of pipes. Here a prime (′) denotes runners connected to the pipes. In this situation, the gas has to choose the preferred direction between pipe 1 and pipe 2 at the dividing point of the runners or the gas injection point. Thus velocities to two directions at this dividing point should be compared. The applied diameters of pipes and runners are given as in Table 3. The rule of thumb of Eq. (35) was modified to include the effect of runners and was used to evaluate the value of the ratio of initial axial velocities in runners (RT) between upper side and lower side. Table 6 provides the values of RT for Figs. 12 to 19. The values of RT turned out to be quite consistent with the results of the simulations for Figs. 12 to 14. However, the values of RT were not consistent with the simulation results (i.e., flow directions) in the cases of Figs. 15 to 19 where they were very close to unity. Since the value of RT was obtained based upon the initial velocities in both sides of runners, the direction of gas flow may be reversed according to the remaining resistances in both sides when the values of RT were very close to unity [Lim and Lee, 2003]. Therefore, the ratio of initial velocities should be recalculated at the first coming change of diameters in both sides (i.e., D_1 and D_{21}) to obtain the corrected ratio of initial velocities (CRT) as in Table 6 when the values of RT are very close to unity. Thus the values of CRT were considered only when the values of RT were close to unity. The flow direction predicted according to the values of CRT was quite consistent with the result of simulation (MOLDFLOW).

CONCLUSION

One may frequently encounter the problem of relatively thick fan-shaped cavity between two square plates where $(H/R_0)^2$ is around 10^{-1} and $\tilde{\theta}^2$ is the order of one. For these conditions the rule of thumb containing a first order-approximated flow model was introduced to show, in qualitative way, whether the resistance of the relatively thick cavity of two square plates may affect the gas direction in GAIM under the aforesaid geometry. Subsequently, various simulations were performed under the conditions that all dimensions of cavity of two square plates and pipes were fixed except for the diameters of pipes and the results of simulation were compared with the results of rule of thumb (RT1) containing the approximated flow model as well as those of another rule of thumb (RT2) without the resistance of the relatively thick cavity of two square plates. RT1 may be used as a criterion to determine where the gas flows earlier between to upper pipes and to lower pipes while RT2 may be used to determine where the gas flows faster between inside upper pipes and inside lower pipes. The results of simulations were generally consistent with the former in a qualitative way to determine gas directions in gas assisted injection molding even though a relatively large value of 0.36 was applied as the value of ε to describe a relatively thick cavity of two square plates. There were some exceptional cases that RT1 or RT2 were not consistent with the simulation results (i.e., flow directions). Both cases may be interpreted as that the gas may not flow to pipes of the side where the gas enters earlier if the gas flows slower in the pipes of that side or may be interpreted as that the gas may flow to pipes of the side where the gas enters earlier even if the gas flows a little bit slower in those pipes, respectively. Thus such a developed model as time-dependent model is required to describe transient behavior of the interface between gas phase and resin phase, which will be treated in part 2 of this paper.

In addition, the situation was treated when cavities of pipes and runners were involved in the configuration. The rule of thumb was used for the ratio of initial velocities to be recalculated at the first coming change of diameters when the ratio was close to unity and it was quite consistent with the results of simulation.

NOMENCLATURE

CRT : corrected ratio of initial velocities at first coming change of diameters in upper side and lower side of Fig. 2b
D : diameter of pipe or conduit
D′ : diameter of a runner
h : distance between top or bottom plate and center-line of the cavity
H : distance between two parallel plates
L : length of pipe in the direction of flow
L′ : length of a runner
P : pressure
P_1 : pressure at $r=R_1$
P′ : pressure at $r=R'$
P_0 : pressure at $r=R_0$
$\tilde{P}$: dimensionless pressure
$\overline{P}$: characteristic pressure
Δp : pressure drop along the distance
Q : flow rate of melt resin
R_1 : radius of nozzle for melt resin- or gas-injection
R_0 : radius of initial polymer shut off
R' : position randomly chosen in r direction between $r=R_1$ and $r=R_0$
RT : ratio of initial axial velocities in runners between upper side and lower side of Fig. 2b
RT1 : ratio of initial resin radial velocities at $r=R_0/2$ of the cavity of two square flat plates connected to upper pipes and lower pipes of Fig. 2a
RT2 : ratio of initial axial velocity of upper pipes and lower pipes neglecting the cavity of two square flat plates of Fig. 2a
r : coordinate in cylindrical coordinate
$\tilde{r}$: dimensinless radial coordinate
r^* : resiatance to the initial velocity of melt polymer at the nearest geometry to a gas injection point
$r^\#$: resistance to Q
$\hat{t}$: characteristic time
$\tilde{t}$: dimensionless time
V : average axial velocity
V^* : initial velocity of melt polymer at the nearest geometry to a gas injection point
V_r : velocity in r direction
V_z : velocity in z direction

$\overline{V}_r$: characteristic velocity in r direction
$\overline{V}_z$: characteristic velocity in z direction
$\tilde{V}_r$: dimensionless radial velocity
$\tilde{V}_z$: dimensionless axial velocity
$\langle V_r \rangle$: average radial velocity
z : coordinate in cylindrical coordinate
$\tilde{z}$: dimensinless axial coordinate

Greek Letters

ρ : density of polymer melt phase
θ : coordinate in cylindrical coordinate
$\hat{\theta}$: vertex angle of the fan-shaped radial flow
$\tilde{\theta}$: dimensionless θ coordinate
μ : newtonian viscosity

Subscripts

1 : upper side
11 : the first pipe at upper side
12 : the second pipe at upper side
2 : lower side
21 : the first pipe at lower side
22 : the second pipe at lower side

REFERENCES

Chen, S.-C., Cheng, N.-T. and Hsu, K.-S., "Simulations and Verification of the Secondary Gas Penetration in a Gas Assisted Injection Molded Spiral Tube," *International Communications in Heat and Mass Transfer*., **22**, 319 (1995).

Chen, S.-C., Cheng, N.-T. and Hsu, K.-S., "Simulations of Gas Penetration in Thin Plates Designed with a Semicircular Gas Channel During Gas Assisted Injection Molding," *Int. J. Mech. Sci*., **38**, 335 (1996a).

Chen, S.-C., Cheng, Hsu, K.-F. and Hsu, K.-S., "Polymer Melt Flow and Gas Penetration in Gas Assisted Molding of a Thin Part with Gas Channel Design," *Int. J. Heat Mass Transfer*, **39**, 2957 (1996b).

Chen, S.-C., Cheng, N.-T. and Chao, S.-M., "Simulations and Verification of Melt Flow and Secondary Gas Penetration During a Gas Assisted Injection Molding," *International Polymer Processing*, **14**, 90 (1998).

Gao, D. M., Nguyen, K. T., Garcia-Rejon, and Salloum, G., "Optimization of the Gas Assisted Injection Moulding Process Using Multiple Gas-injection Systems," *Journal of Materials Processing Technology*, **69**, 282 (1997).

Khayat, R. E., Derdouri, A. and Herbert, L. P., "A Three-dimensional Boundary-element Approach to Gas Assisted Injection Molding," *J. Non-Newtonian Fluid Mech*., **57**, 253 (1995).

Lim, K. H., "Flow Direction when Fan Shaped Geometry is Applied in Gas Assisted Molding: 1. Theory of Flow Model and its Criterion to Predict Flow Directions," *Korean J. Chem. Eng*., **21**, 48 (2004a).

Lim, K. H., "Gas Flow Direction Under Heterogeneous Geometry Composed of a Pipe and a Cavity of Two Square-flat Plates in Gas Assisted Injection Molding," *Journal of Industrial and Engineering Chemistry*, **10**(3), 416 (2004b).

Lim, K. H. and Hong, S. H., "Flow Direction when Fan Shaped Geometry is Applied in Gas Assisted Molding: 2. Development of Flow Model and its Predictions," *Korean J. Chem. Eng*., **21**, 59 (2004).

Lim, K. H. and Lee, E. J., "Predictions of Gas Flow Directions in Gas Assisted Injection Molding when Cavities and Runners are Involved," *Korean J. Chem. Eng.*, **20**(3), 592 (2003).

Lim, K. H. and Soh, Y. S., "The Diagnosis of Flow Direction under Fan Shaped Geometry in Gas Assisted Injection Molding," *Journal of Injection Molding Technology*, **3**, 31 (1999).

McCabe, W. L., Smith, J. C. and Harriot, P., "Unit Operations of Chemical Engineering," 4th Ed., McGraw-Hill Press (1986).

Parez, M. A., Ong, N. S., Lam, Y. C. and Tor, S. B., "Gas-assisted Injection Molding: The Effects of Process Variables and Gas Channel Geometry," *Journal of Material Processing Technology*, **121**, 27 (2002).

Shen, Y. K., "Study on the Gas-liquid Interface and Polymer Melt Front in Gas Assisted Injection Molding," *Int. Comm. Heat Mass Transfer*, **24**, 295 (1997).

Shen, Y. K., "Study on Polymer Melt Front, Gas Front and Solid Layer in Filling Stage of Gas Assisted Injection Molding," *Int. Comm. Heat Mass Transfer*, **28**, 139 (2001).

Soh, Y. S. and Lim, K. H., "Control of Gas Direction in Gas Assisted Injection Molding; Definition of Resistance to Velocity," *SPE ANTEC Tec. Papers*, **60**, 482 (2002).

Soh, Y. S., "Control of Gas Direction in Gas Assisted Injection Molding," *Journal of Reinforced Plastics and Composites*, **19**, 955 (2000).

Soh, Y. S. and Chung, C. H., "Flow Directions in the Gas Assisted Injection Technology," *Journal of Reinforced Plastics and Composites*, **17**, 935 (1998).